Available online at www.sciencedirect.com
SCIENCE DIRECT®
Mechanics of Materials 35 (2003) 1149–1159
MECHANICS OF MATERIALS
www.elsevier.com/locate/mechmat

Molecular reorganization in wood

Petri P. Kärenlampi *, Pekka Tynjälä, Pasi Ström

Faculty of Forestry, University of Joensuu, P.O. Box 111, Joensuu FIN-80101, Finland

Received 28 May 2002; received in revised form 25 November 2002

Abstract

Cyclical compression was applied to steamed Spruce wood in uniaxial strain under stress control. Molecular fatigue response was investigated in terms of thermoporosimetry. In accordance with classical Coffin–Manson theory, it was found that the creation of fatigue damage depends on plastic strain amplitude, not depending on the applied stress, applied strain, or the amount of dissipated energy as such. At a specified strain amplitude, molecular fatigue does not appear to be sensitive to loading frequency. However, it does appear to be related to decrement of dynamic stiffness in the course of dynamic loading. Molecular reorganization becomes more pronounced along with further energy application. Results for specimens loaded in the tangential material direction are rather consistent, whereas the molecular reaction varies widely along with the local strain amplitude in the case of specimens loaded in the radial material direction. This implies that the molecular fatigue process is essentially strain-controlled, rather than stress-controlled.

Keywords: Cell wall porosity; Thermoporosimetry; Molecular fatigue; Strain level; Strain amplitude; Energy dissipation; *Picea Abies*

1. Introduction

Wood is an anisotropic composite of polymeric constituents. It is widely available, and used for a variety of purposes, including constructions, joinery, pulp and paper, as well as for dissolving to chemicals. A variety of such industries apply steam treatment as a process means, just to mention moisture and temperature softening of joinery components, as well as steaming of wood in the context of mechanical and chemical pulping. The mechanical properties of steam-treated wood are of interest in all those industries which combine steam treatment with mechanical action. Mechanical pulping processes essentially consist of fatigue treatments, intending to loosen the internal structure of steam-treated wood.

Wood is a rather complex composite of polymeric constituents. The different constituents, cellulose, hemicelluloses and lignins, display significantly different properties. In the abundance of water, hemicelluloses tend to soften below room temperature, where lignins and cellulose remain stiff (Kersavage, 1973; Cousins, 1977, 1978; Salmén, 1984, 1993). A widely accepted hypothesis is that the softening of lignins largely dominates the effect of temperature and moisture on time-dependent mechanical behavior of wood, at least in the range

* Corresponding author. Tel.: +358-13-251-4009; fax: +358-13-251-3590.
E-mail address: petri.karenlampi@joensuu.fi (P.P. Kärenlampi).

0167-6636/$ - see front matter
doi:10.1016/S0167-6636(03)00003-6

of moisture and temperature applicable in industrial steaming operations (Salmén, 1984; Irvine, 1985).

Wood is a highly anisotropic composite. A tree bole is in coarse terms cylindrical, and displays rotational symmetry with respect to the central axis. The cellulose microfibrils are mainly oriented in the longitudinal direction. Mechanical stiffness is much higher in the direction of the cellulose microfibrils than in the transverse directions. The cellulose is less susceptible to thermal and moisture-induced softening than the surrounding matrix of hemicellulose and lignin, and thus increasing temperature and moisture in general increase mechanical anisotropy (Kersavage, 1973; Cousins, 1977, 1978; Salmén and Fellers, 1981; Björkqvist et al., 1998; Page and Schulgasser, 1989).

Stress–strain behavior of cellular materials in general is non-linear (Gibson and Ashby, 1988; Christensen, 2000). In particular, *radial* and *tangential* compression of wood first display an apparently linear elastic range, after which strain can be increased without any major increment of stress (Bodig, 1965; Easterling et al., 1982; Gril and Norimoto, 1993; Uhmeier, 1995; Uhmeier and Salmén, 1996a,b). This "plateau region" is likely to be due to buckling of cell walls into the cell lumens (March and Smith, 1945; Bodig, 1965; Kunesh, 1967; Easterling et al., 1982; Uhmeier, 1995; Bienfait, 1926; Kitahara et al., 1981). Once the strain becomes that large that the space in the lumens available for cell wall buckling becomes limited, the compressive stress again starts to significantly increase as a function of increasing compressive strain (Easterling et al., 1982; Gril and Norimoto, 1993; Uhmeier, 1995; Uhmeier and Salmén, 1996a,b). Short-time mechanical behavior of wood may significantly depend on the degree of hydraulic filling of the lumens (Gibson and Ashby, 1988; Uhmeier, 1995).

The stress–strain compression behavior of wood in the longitudinal direction has been observed to differ significantly from the stress–strain behavior in the transverse directions, the longitudinal direction showing instabilities at strains of a few per cent, manifested as decrement of stress as a function of increasing strain (Easterling et al., 1982; Kärenlampi et al., 2001). Longitudinal instability appears to depend not only on stress but also on loading time, as well as the number of applied loading cycles (Bach, 1979; Clorius et al., 2000).

Consisting of amorphous polymers, wood displays time-dependent mechanical behavior. However, at least up to 100 °C, 50% compressive engineering strain in the radial direction, and straining time of a few seconds, true irrecoverable (plastic) deformation in wood has been found to be small (Uhmeier, 1995; Uhmeier and Salmén, 1996a). Thus, at least in radial compression, wood appears to behave viscoelastically. However, there is no definite reason to assume that the mechanical response would still be viscoelastic in other material directions, greater temperatures, and with longer straining times (Keith, 1972; Kärenlampi et al., 2001; Kärenlampi, 2001a).

The mechanical behavior of steamed wood under cyclical compression has been recently investigated (Kärenlampi et al., 2002a,b). Investigations have shown that even though the mechanical behavior in terms of energy dissipation, strain amplitude and dynamic stiffness is rather sensitive to stress level and stress amplitude, the decrement of small-strain stiffness has been an almost unique function of the level of greatest compressive strain which has appeared during loading (Kärenlampi et al., 2002b,c). The stiffness decrement has been closely related to plastic strain (Kärenlampi et al., 2002a,b,c). Thus such measures have not appeared to reflect the variety of material reactions to fatigue treatments.

In heterogeneous hydrated systems, the amount of water with depressed melting temperature is detectable using Differential Scanning Calorimetry (DSC) (Rennie and Clifford, 1977; Homshaw, 1981; Ishikiriyama and Todoki, 1995). The depressed melting temperature can be interpreted either as a consequence of some material constituents being partially solubilized or the material being microporous in such a way that surface tension of pure water depresses the melting temperature of water, due to the small pore radius (Maloney et al., 1998). The latter interpretation enables porosity investigation in terms of thermoposimetry (Maloney, 1999; Maloney et al., 1998; Maloney and Paulapuro, 1999).

The porosity of the wood fiber cell wall increases along with decreasing yield in the course of chemical pulping (Stone and Scallan, 1967; Stone et al., 1968; Maloney and Paulapuro, 1999; Scallan, 1978), and increases in the course of mechanical pulping and chemical pulp beating (Maloney and Paulapuro, 1999; Scallan, 1978; Stone et al., 1968; Salmén et al., 1985). It has been recently shown that the cell wall porosity significantly evolves along with wood basic density, as a function of position within an annual ring (Tynjälä and Kärenlampi, 2001).

In this paper, we will investigate dynamic mechanical behavior of Spruce wood, steam-treated at 130 °C. In particular, we will explore the molecular response of specimens subjected to compressive fatigue loading in unidirectional strain. First, we will describe experimental arrangements. Then, we will report the evolution of compressive strain and dynamic stiffness the course of cyclical compressive loading, and address the energy dissipation during such loading. Finally, the effect of process variables on the changes in cell wall porosity in the nanometer scale will be reported.

2. Materials and methods

Spruce heartwood specimens of dimensions $34 \times 34 \times 9$ mm and of dry mass 4.0 g ($\pm 5\%$), frozen as fresh and then melted in water overnight, were treated with saturated water steam at 130 °C. After steaming of 40 min, experiments were conducted by compressing any specimen in uniaxial strain in the direction of 9 mm thickness.

A previous investigation (Kärenlampi et al., 2002c) has shown a stress–strain behavior for specimens of the present kind as shown in Fig. 1. Engineering stress as a function of logarithmic strain (''true strain'') under monotonically increased compressive strain at rate 5%/s is shown. After reaching 80% compressive strain, the strain was released under strain control, using the same strain rate. We find that the stress–strain behavior was highly nonlinear in the radial and tangential material directions; there was a wide range of strain where the compressive stress increased only slightly as a function of increasing compressive strain. This significant yielding starts at a yield stress of approximately 0.4 MPa. The radial and tangential material directions do not distinguish themselves dramatically from each other; however, at a specified strain the radial material direction displays greater compressive stress at small strains. The compressive strains exceeding 5%, the tangential compressive stress is greater (Kärenlampi et al., 2002a,c).

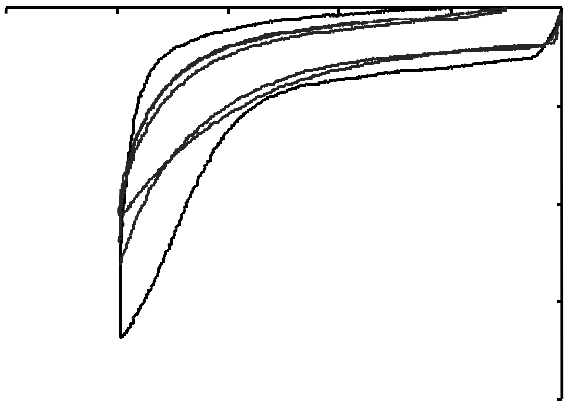

Fig. 1. Stress–strain behavior of specimens in first-time compression applied in radial and tangential material directions.

Any dynamic test was here conducted by applying a sinusoidal stress of constant set point and amplitude. Fig. 1 was used in the selection of the applied stress scale. It was recognized that in the case of dynamic loading experiments with a duration of a few seconds, stress levels not exceeding the yield stress do not induce much of material fatigue. First, the peak compressive stress was selected as three times the initial stress level of 0.4 MPa, resulting as 1.2 MPa. In order to experiment with a greater stress, a peak compressive stress of 2.7 MPa was used.

Two levels of relative double amplitude of stress were used. The double amplitude in relation to peak compressive stress was taken as either 30% or 90%. In other words, either 30% or 90% of applied compressive stress was released within any loading cycle. An example of such a dynamic loading experiment is shown in Fig. 2: peak compressive stress level of 1.2 MPa is applied, and 90% of this compressive stress is released within any cycle. The strain level evolves while the experiment proceeds.

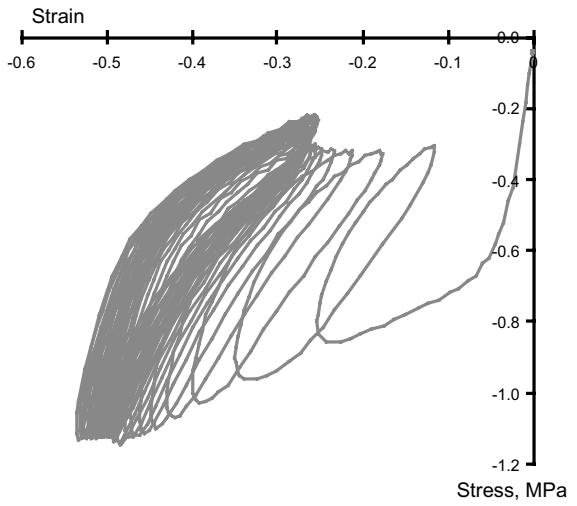

Fig. 2. First stress–strain cycles in a dynamic loading experiment with 1.2 MPa compressive peak stress and 90% relative stress amplitude.

We also find that a few stress cycles have to be implemented before the instrumentation succeeds in stabilizing the stress variation to the desired range.

The dynamic testing program, applied in the tangential material direction, is shown in Table 1. Table 1 also reports the amount of mechanical work applied to any specimen, as well as the amount of energy dissipated within any test; energy which did not recover within release of compressive strain was considered as dissipated. The energy application target for any specimen was 10 MJ/m^3, except the two last specimens in Table 1, where an energy application of 20 MJ/m^3 was intended.

Table 1
The dynamic loading program

Peak compressive stress (MPa)	Double stress amplitude (MPa)	Loading frequency (Hz)	Number of cycles	Applied energy (MJ/m^3)	Dissipated energy (MJ/m^3)
1.2	1.0	10	120	15	5.1
1.2	1.0	10	120	11	3.6
1.2	1.0	10	120	13	4.6
2.7	0.8	10	600	6.6	0.9
2.7	0.8	10	900	9.5	1.1
2.6	2.2	10	90	8.6	3.0
2.6	2.3	10	100	9.1	3.2
2.6	2.2	100	140	11	4.5
2.7	2.4	100	140	7.3	3.0
2.7	2.4	100	140	6.7	2.9
2.7	2.4	100	380	20	8.3
2.6	2.3	100	500	24	10

After dynamic loading, an earlywood specimen of dry mass 5 mg was produced from any of the loaded specimens. Any small earlywood specimen, along with 10 mg of deionized water, was placed in a DSC within 15 min from the termination of dynamic loading, and frozen to −45 °C. Then, the temperature was increased to +25 °C, and the amount of melting water was determined through the measurement of melting enthalpy. The total amount water within the specimen was determined through drying the specimen and deducting the dry mass from the total mass. The distinction between the total amount of water and the melting water was taken as the amount of non-freezing water (NFW). In accordance with the Gibbs–Thompson equation, it was assumed that water in pores which are small enough does not freeze at −45 °C, and the amount of NFW within a specimen in relation to the dry mass of the specimen was taken as a measure of porosity in the nanometer scale.

3. Evolution of strain

The evolution of strain level within any test is shown in Fig. 3. This figure displays the greatest compressive (logarithmic) strain detected within any loading cycle. We find that the strain level is a function of stress level. Compressive strain levels induced by loading up to 2.7 MPa of compressive stress are greater than strain levels induced by compressive stresses up to 1.2 MPa.

Stresses up to 1.2 MPa applied at 10 Hz loading frequency induce a significant evolution of compressive strain in the course of any test. Stresses up to 2.7 MPa also induce an evolution of strain level, which however is less pronounced since the greater stress instantly induces a compressive strain exceeding 70%. With 2.7 MPa compressive peak stress, the strain level at a specified energy application is greater with 30% double stress amplitude than in the case of 90% double stress amplitude. A

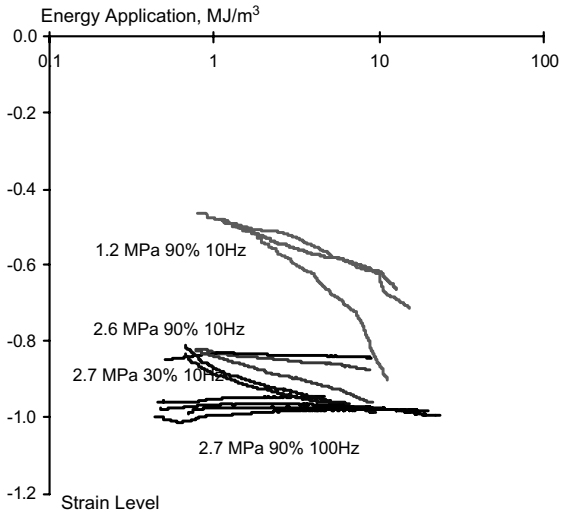

Fig. 3. Strain level as a function of applied energy during dynamic loading. Curves are labeled according to greatest applied compressive stress level, relative double stress amplitude, and loading frequency.

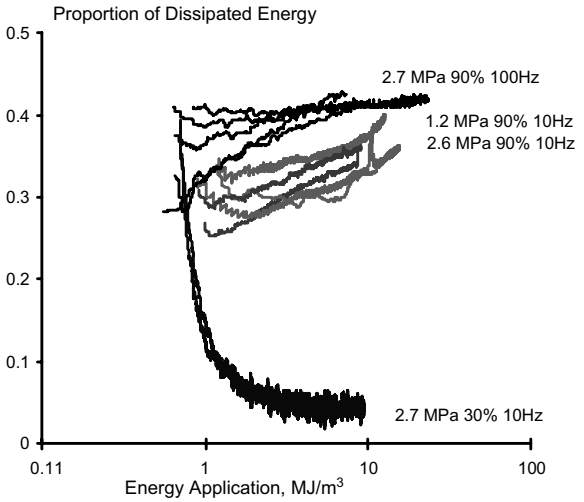

Fig. 4. Proportion of dissipated energy as a function of applied energy during dynamic loading. Curves are labeled according to greatest applied compressive stress level, relative double amplitude of stress, and loading frequency.

natural explanation is that the smaller relative amplitude results as greater average compressive stress.

Somewhat surprisingly, the compressive strain level does not increase in the course of cyclical loading at 100 Hz frequency. There rather appears to be a slight strain recovery during dynamic loading. The absence of increment of compressive strain level may be partly due to the brief duration of such a high-frequency treatment. Another reason may be that in order to avoid instability of stress in the high-frequency test, it was necessary to introduce a stress ramp of 3 s up to the desired compressive peak stress prior to dynamic loading. Quite a high compressive strain appeared already during the stress ramp. The minor strain recovery may be due to some overload appearing in the beginning of the technical implementation of such a high-frequency test, despite of the previously applied stress ramp.

4. Energy dissipation

The proportion of applied energy not recovered within three consecutive loading cycles is shown in Fig. 4. We find that the specimens loaded with 30% relative stress amplitude significantly differ from the specimens loaded with 90% relative stress amplitude. After energy dissipation associated to the initial increment of compressive strain (cf. Fig. 3), the behavior of specimens loaded with the small relative amplitude is almost elastic, whereas 30–40% of the energy applied at 90% relative stress amplitude becomes dissipated, regardless of the applied peak stress.

Fig. 4 further shows that in the case of 90% relative stress amplitude, the energy dissipation rate somewhat increases along with energy application. The energy dissipation rate is the greater the greater the loading frequency. At constant relative stress amplitude and loading frequency, the energy dissipation rate appears to be independent of the applied stress level.

5. Dynamic stiffness

Dynamic stiffness, defined as the ratio of stress amplitude to strain amplitude during dynamic loading, is shown as a function of energy application in Fig. 5. We find that the greater is the applied stress, the greater is the dynamic stiffness.

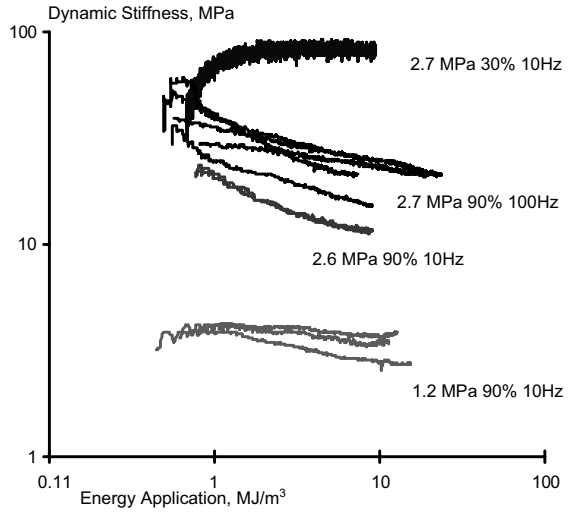

Fig. 5. Dynamic stiffness as a function of applied energy in dynamic loading. Curves are labeled according to greatest applied compressive stress level, relative double amplitude of stress, and loading frequency.

This also applies to experiments with similar peak stress but different stress amplitude: in the case of 30% relative double amplitude of stress, the mean stress is greater, and dynamic stiffness is greater than in the case of 90% relative double stress amplitude.

We find from Fig. 5 that in the case of specimens loaded at 90% relative double amplitude of 2.7 MPa compressive peak stress, the dynamic stiffness deteriorates along with energy application. This hardly is solely due to the increment of temperature, since the stiffness of specimens loaded with 1.2 MPa compressive peak stress deteriorates less, even though such specimens dissipate the same amount of energy (cf. Fig. 4). It thus appears likely that the deterioration of stiffness reflects structural damage.

Specimens loaded with 2.7 MPa compressive peak stress and 90% relative stress amplitude show a greater dynamic stiffness at 100 Hz loading frequency than at 10 Hz loading frequency (Fig. 5). Thus we find that the dynamic stiffness appears to be is the greater the greater the loading frequency. This observation is in accordance with general knowledge regarding the time-dependent mechanical properties of amorphous polymers (Williams et al., 1955; Ferry, 1961; Smith, 1962).

6. Molecular fatigue

The NFW content of moist, virgin Spruce earlywood has been reported to be 16–20% of the dry mass of the wood (Tynjälä and Kärenlampi, 2001). Within the present investigation it was verified that the same applies to steam-treated earlywood in the absence of any mechanical fatigue loading. The NFW content reflecting cell wall porosity in the nanometer scale, it is here assumed to reflect microstructural damage due to mechanical treatment.

Previous investigations have shown that plastic strain, as well as decrement of small-strain stiffness modulus, due to mechanical compression fatigue treatment, is due to the greatest compressive strain which has appeared during loading, being insensitive to the details of the mechanical treatment (Kärenlampi et al., 2002b,c). However, the present results show that molecular fatigue, reflected in the NFW content, is not dictated by the greatest strain applied during loading.

We find from Fig. 6 that specimens being loaded with 2.7 MPa compressive peak stress and 30% relative double stress amplitude have experienced the same compressive strain as specimens loaded with 90% relative double stress amplitude.

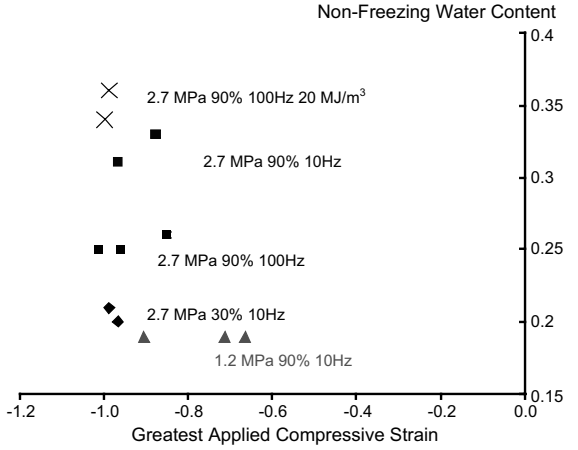

Fig. 6. Nanometer-scale porosity as a function of greatest applied compressive strain. Observations are labeled according to greatest applied compressive stress level, relative double amplitude of stress, and loading frequency. Treatments extended to 20 MJ/m^3 energy input are indicated.

The low-amplitude experiments however show only a very small increment in the NFW content, whereas the molecular fatigue in specimens treated with greater relative amplitudes is rather pronounced.

Energy dissipation has been proposed as a measure of the efficiency of wood fatigue treatment (Höglund et al., 1976; Becker et al., 1977). We find from Fig. 7 that specimens subjected to 20 MJ/m^3 energy application have dissipated most energy, and they also have shown most of molecular reorganization. However, considering the specimens subjected to an energy application in the order of 10 MJ/m^3, there does not appear to be much dependency between energy dissipation and porosity changes. Specimens loaded up to 1.2 MPa compressive stress show the greatest energy dissipation but the least NFW content. On the other hand, specimens loaded with 30% relative double stress amplitude show a small amount of dissipation but still a small NFW content.

Seminal observations regarding the thermal fatigue of metals have related the extent of fatigue damage to cyclical inelastic strain (Coffin, 1954; Manson, 1954; Suresh, 1998; Kärenlampi, 2001b). Thus it appears reasonable to discuss inelastic strain amplitude as a fatigue process parameter.

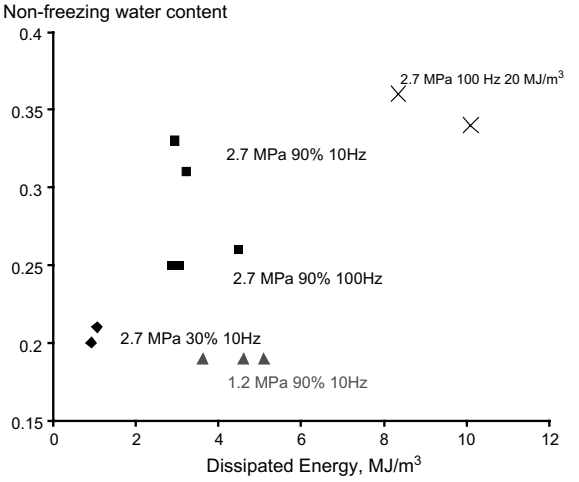

Fig. 7. Nanometer-scale porosity as a function of dissipated energy. Observations are labeled according to greatest applied compressive stress level, relative double amplitude of stress, and loading frequency. Treatments extended to 20 MJ/m^3 energy input are indicated.

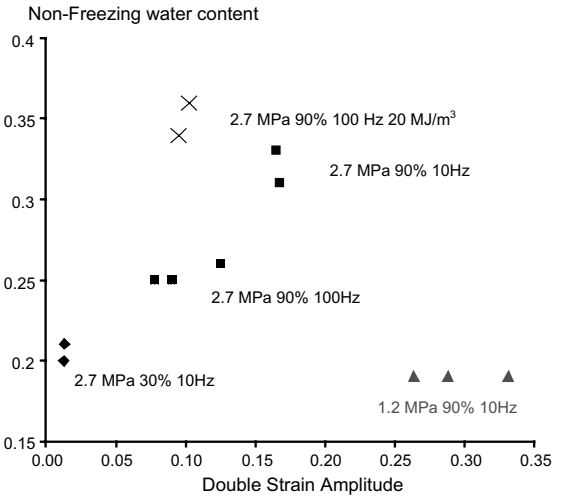

Fig. 8. Nanometer-scale porosity as a function of double strain amplitude. Observations are labeled according to greatest applied compressive stress level, relative double amplitude of stress, and loading frequency. Treatments extended to 20 MJ/m^3 energy input are indicated.

Fig. 8 shows the NFW content as a function of the mean value of total double strain amplitude which occurred within any treatment.

Specimens loaded with peak stress 1.2 MPa show the greatest strain amplitudes. These specimens do not show any molecular reorganizations. It is not know to which degree the cyclical strain within the earlywood has been locally inelastic at this stress level.

With compressive peak stress of 2.7 MPa and 10 MJ/m^3 energy application, the NFW content within treated specimens appears to be linearly related to the strain amplitude. 30% relative double stress amplitude, leading to 1% double strain amplitude, reorganized the structure of earlywood cell walls negligibly. Ninenty percentage relative double stress amplitude, leading to 17% double strain amplitude, resulted as an NFW content of 31–33%. Increasing the loading frequency to 100 Hz reduced the double strain amplitude to the vicinity of 10%, and the NFW content to 25–26%.

Specimens given 20 MJ/m^3 of energy application show the greatest molecular reactions. Thus it appears that further treatment enhances molecular reorganization. In other words, fatigue damage

accumulates along with further work. The mean strain amplitude at the 20 MJ/m^3 energy application level appears slightly higher than in the case of similarly loaded specimens at the 10 MJ/m^3 energy application level.

7. Discussion

Cyclical compression was applied to steamed Spruce wood in uniaxial strain under stress control. Molecular fatigue response was investigated in terms of thermoporosimetry.

Previous investigations have shown that even though the mechanical behavior in terms of energy dissipation, strain amplitude and dynamic stiffness is rather sensitive to stress level and stress amplitude, the decrement of small-strain stiffness has been an almost unique function of the level of greatest compressive strain which has appeared during loading (Kärenlampi et al., 2002b). The stiffness decrement has been closely related to plastic strain (Kärenlampi et al., 2002b,c). Thus such measures have not appeared to reflect the variety of material reactions to fatigue treatments.

Nanometer-scale porosity does appear to reflect the variety of material reactions to fatigue treatments. At constant compressive peak stress of 2.7 MPa and at energy application level of 10 MJ/m^3, the extent of molecular reorganizations appeared to be linearly related to strain amplitude (Fig. 8). This effect was similar regardless whether the strain amplitude was changed through changing stress amplitude or through changing loading frequency.

Specimens loaded at compressive peak stress 1.2 MPa did not show any molecular fatigue reactions, despite significant energy dissipation (Figs. 4 and 7) and large strain amplitude (Fig. 8). In terms of high-cycle fatigue concepts, an obvious explanation is that at this stress level, most of the cyclical deformation was elastic, not leading to significant kinematic irreversibility. Compressive peak stresses of 2.7 MPa in turn did appear to induce kinematic irreversibility. It would be of interest to investigate whether peak stresses greater than 2.7 MPa would further accelerate the accumulation of fatigue damage.

Specimens loaded at compressive peak stress 2.7 MPa with 30% relative double stress amplitude did not show much molecular fatigue reactions, despite the significant stress level and considerable compressive strain accumulation (Figs. 3 and 6). An obvious explanation is the very small strain amplitude resulting from these process conditions (Fig. 8).

It appeared that those process conditions leading to significant increment of nanometer-scale porosity also induced a decrement in dynamic stiffness, appearing in the course of fatigue loading (Figs. 5 and 8). Specimens with 1.2 MPa compressive peak stress showed less decrement in dynamic stiffness, regardless of significant energy dissipation (Figs. 4 and 5). Thus the decrement in dynamic stiffness appears to reflect not only increment of temperature, but also molecular reorganization.

The deterioration of stiffness reflecting structural damage, extended fatigue treatment obviously should increase the NFW content. This is seen in Figs. 6–8: specimens given a fatigue treatment of 20 MJ/m^3 energy application showed the greatest amount of molecular (or fibrillar) reorganization.

It might be instructive to consider how the molecular reorganization possibly would be affected by a change in process temperature. In amorphous polymers, molecular mobility increases with increasing temperature (Williams et al., 1955; Ferry, 1961; Smith, 1962). Thus one can assume that decrement of temperature would reduce the amount of molecular reorganization.

The effect of temperature on molecular reorganization is shown in Fig. 9. We find that decrement of process temperature to 100 °C reduces the resulting NFW content from 32% to 26%, the mechanical treatmens being similar with 2.7 MPa peak compressive stress, 90% relative stress amplitude and 10 Hz loading frequency. In analogy with Fig. 8, the amount of molecular reorganization increases with increased energy application: 30 MJ/m^3 at 100 °C results as the same NFW content as 10 MJ/m^3 at 130 °C (Fig. 9). With constant stress amplitude, the strain amplitude is greater at the lower temperature (Fig. 9).

The effect of (plastic) strain amplitude on the NFW content appears from Fig. 8 to be even

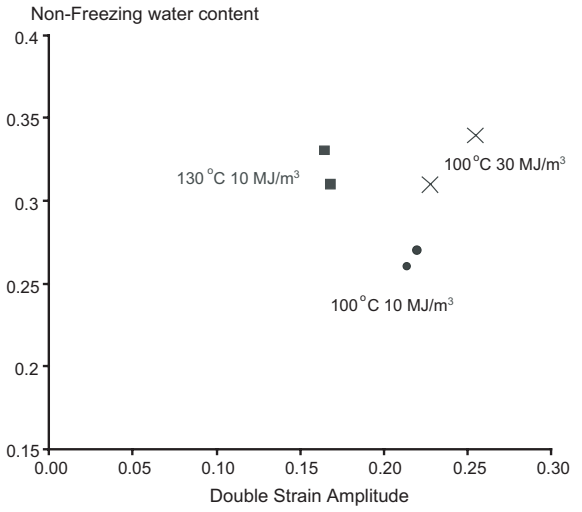

Fig. 9. Nanometer-scale porosity as a function of double strain amplitude, specimens being loaded with 2.7 MPa peak compressive stress, 90% relative double amplitude of stress, and 10 Hz loading frequency. Observations are labeled according to applied process temperature and amount of mechanical energy application.

surprisingly consistent. This may be due to the specimens being loaded in the tangential direction. Wood displays a significant millimeter-scale periodic variation in structure and properties in the radial direction, the different phases of this variation often being denoted as "earlywood" and "latewood". The specimens have been loaded in the tangential material direction, and thus perpendicular to the waves of periodicity. Thus the strain and the strain amplitude have been rather uniform within the specimen, whereas the stress and the stress amplitude have varied along with the periodic variation in material properties.

In the case of specimens loaded in the radial material direction, the loading direction would be along the waves of the periodic variation in material properties. Under such loading circumstances the strain and the strain amplitude would vary widely within any annual ring, whereas the stress and the stress amplitude would be rather uniform.

The consistency of the results shown in Fig. 8 proposes that the molecular fatigue process is essentially strain-driven, in accordance with the high-cycle fatigue approach by Coffin (1954) and Manson (1954). Alternatively, one might think of a stress-controlled, low-cycle fatigue process (Suresh, 1998). It is possible to clarify the eventual validity of the low-cycle fatigue approach by briefly investigating the eventual scatter of NFW content in the case of some specimens dynamically loaded in the radial material direction.

Fig. 10 shows the NFW content of specimens loaded with 2.7 MPa peak compressive stress and 90% relative double stress amplitude in the radial direction. Thus the stress level and the stress amplitude have been the same in all the experiments. Two different loading frequencies have been used. Thus the variation in strain amplitude is mostly due to time-dependency of dynamic stiffness.

We find from Fig. 10 that there is a very significant scatter of NFW content within any loading frequency. The variation in the molecular response to any specified kind of dynamic loading is far greater than in Fig. 8. Thus the principal variation of strain amplitude appears to induce a great variation in the molecular response (Fig. 10). On the other hand, some variation in the stress amplitude provides results which are rather

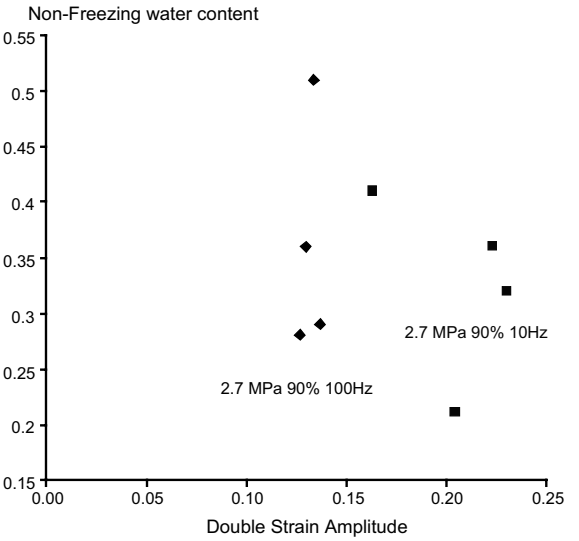

Fig. 10. Nanometer-scale porosity as a function of apparent double strain amplitude, specimens being loaded in the radial material direction. Observations are labeled according to greatest applied compressive stress level, relative double amplitude of stress, and loading frequency.

consistent as long as the strain amplitude is basically invariant (Fig. 8).

It is worth noting that the molecular response to dynamic loading has here been discussed in terms of the NFW content of 5 mg earlywood specimens. The NFW content of latewood differs from that of earlywood, and the effect of some treatments are quite different (Tynjälä and Kärenlampi, 2001). The effect of dynamic loading on latewood remains to be investigated.

Acknowledgements

The authors are obliged Tomas Björkqvist for commenting on the manuscript, and to the National Technology Agency of Finland for financing.

References

Bach, L., 1979. Frequency-dependent fracture in wood under pulsating loading. In: Forest Products Research Society Annual Meeting 1975, June 15, Portland, OR, 33 p. (The Technical University of Denmark, Department of Civil Engineering, Building Materials Laboratory, Technical Report 68/79).

Becker, H., Höglund, H., Tistad, G., 1977. Frequency and temperature in chip refining. Pap. Puu 59 (3), 123–130.

Bienfait, J.L., 1926. Relation of the manner of failure to the structure of wood under compression parallel to the grain. J. Agric. Rec. 33 (2), 183–194.

Björkqvist, T., Liukkonen, S., Lucander, M., Saharinen, E., 1998. Kuidutuspinnan ja puun tehokkaampi vuorovaikutus (KUPU). Loppuraportti. Tampere University of Technology, Automation and Control Institute, Report 4/1998.

Bodig, J., 1965. The effect of anatomy on the initial stress–strain relationship in transverse compression. Forest Prod. J., 15, 197–202.

Christensen, R.M., 2000. Mechanics of cellular and other low-density materials. Int. J. Solids Struct. 37, 93–104.

Clorius, C.O., Pedersen, M.U., Hoffmeyer, P., Damkilde, L., 2000. Compressive fatigue in wood. Wood Sci. Technol. 34, 21–37.

Coffin, L.F., 1954. A study on the effect of cyclic thermal stresses on a ductile metal. Trans. Am. Soc. Mech. Eng. (ASME) 76, 931–950.

Cousins, W.J., 1977. Elasticity of isolated lingin: Young's modulus by a continuous indentation method. New Zeal. J. Forestry Sci. 7 (1), 107–112.

Cousins, W.J., 1978. Young's modulus of hemicellulose as related to moisture content. Wood Sci. Technol., 12, 161–167.

Easterling, K.E., Harrysson, R., Gibson, L.J., Ashby, M.F., 1982. On the mechanics of Balsa and other woods. Proc. R. Soc. London A 383, 31–41.

Ferry, J.D., 1961. Viscoelastic properties of polymers. John Wiley and Sons, New York, NY.

Gibson, L.J., Ashby, J.B., 1988. Cellular solids. Pergamon Press, Oxford.

Gril, J., Norimoto, M., 1993. Compression of wood at high temperature. In: Birkinshaw, C., Morlier, P., Seoane, I. (Eds.), COST 508—Wood mechanics, workshop on wood: plasticity and damage. CEC, pp. 135–143.

Homshaw, L.G., 1981. Calorimetric determination of porosity and pore size distribution (PSD): effect of heat on porosity, pore form, and PSD in water-saturated polyacrylonitrile fibers. J. Colloid Interface Sci. 84 (7), 127–140.

Höglund, H., Sohlin, U., Tistad, G., 1976. Physical properties of wood in relation to chip refining. Tappi 59 (6), 144–147.

Irvine, G.M., 1985. The significance of the glass transition of lignin in thermomechanical pulping. Wood Sci. Technol. 19, 139–149.

Ishikiriyama, K., Todoki, M., 1995. Pore size distribution measurements of silica gels by means of differential scanning calorimetry. J. Colloid Interface Sci. 171 (1), 103–111.

Keith, C.T., 1972. The mechanical behavior of wood in longitudinal compression. Wood Sci. 4 (4), 234–244.

Kersavage, P.C., 1973. Moisture content effect on tensile properties of individual Douglas-fir latewood tracheids. Wood & Fiber 5 (2), 105–117.

Kitahara, R., Tsutsumi, J., Matsumoto, T., 1981. Observations on the cell wall response and mechanical behavior in wood subjected to repeated static bending load. Mok. Gakkai. 27 (1), 1–7.

Kunesh, R.H., 1967. Strength and elastic properties of wood in transverse compression. Forest Prod. J. 18 (1), 65–72.

Kärenlampi, P.P., 2001a. Viscoplasticity of steam-treated wood. Submitted (October 2, 2001).

Kärenlampi, P.P., 2001b. The effect of material disorder on fatigue damage induced by unidirectional loading. In: Gualgliano, M., Aliabadi, M.H. (Eds.), Advances in Fracture and Damage Mechanics II. Milan, Italy, September 18–20, 2001, pp. 87–92.

Kärenlampi, P.P., Tynjälä, P., Ström, P., 2001. Mechanical behavior of steam-treated spruce wood under compressive strain. Submitted (10/2001).

Kärenlampi, P.P., Tynjälä, P., Ström, P., 2002a. Dynamic mechanical behavior of steam-treated wood. Mech. Mater. 34 (6), 333–347.

Kärenlampi, P.P., Tynjälä, P., Ström, P., 2002b. Off-axis fatigue loading of steamed wood. Int. J. Fatigue 24 (12), 1235–1242.

Kärenlampi, P.P., Tynjälä, P., Ström, P., 2002c. The effect of temperature and compression on the mechanical behavior of steam-treated wood. J. Wood Sci., in press.

Maloney, T.C., Paulapuro, H., Stenius, P., 1998. Hydration and swelling of pulp fibres measured with differential

scanning calorimetry. Nordic Pulp Paper Res. J. 13 (1), 31–36.

Maloney, T.C., Paulapuro, H., 1999. The formation of pores in the cell wall. J. Pulp Paper Sci. 25 (12), 430–436.

Maloney, T.C., 1999. Thermoporosimetry by isothermal step melting. In: Proc. Pre-Symposium of the 10th ISWPC, Seoul, pp. 245–253.

Manson, S.S., 1954. Behavior of materials under conditions of thermal stress. National Advisory Commission on Aeronautics: Report 1170. Lewis Flight Propulsion Laboratory, Cleveland, OH.

March, H.W., Smith, C.B., 1945. Buckling loads of flat sandwich panels in compression. Various types of edge conditions. D.S.D.A. Forest Service, Forest Prods. Lab., Madison, WI., Report 1525 (March 1945).

Page, D.H., Schulgasser, K., 1989. Evidence for a laminate model for paper. In: Mechanics of Cellulosic and Polymeric Materials. American Society of Mechanical Engineers, New York, pp. 35–39.

Rennie, G.K., Clifford, J., 1977. Melting of ice in porous solids. J. Chem. Soc. F1 73 (4), 680–689.

Salmén, L., 1984. Viscoelastic properties of in situ lignin under water-saturated conditions. J. Mater. Sci. 19 (9), 3090–3096.

Salmén, L., 1993. Responses of paper properties to changes in moisture content and temperature. In: Tenth Fundamental Research Symposium, Oxford 1993. Pira International, Letherhead, UK, pp. 369–430.

Salmén, L., Fellers, C., 1981. The fundamentals of energy consumption during viscoelastic and plastic deformation of wood. In: 1981 International Mechanical Pulping Conference, EUCEPA, Oslo June 16–19, Session VI, Paper 1, 21 p.

Salmén, L., Tigerström, A., Fellers, C., 1985. Fatigue of wood-characterization of mechanical defibration. J. Pulp Paper Sci. 11 (3), J68–73.

Scallan, A.M., 1978. The accommodation of water within pulp fibers. In: 6th Fundamental Research Symposium 1977, (Fiber–Water Interactions in Papermaking), London, 9–29.

Smith, T.L., 1962. Stress–strain–time–temperature relationship for polymers. In: ASTM Materials Science Series 3, STP-325. American Society of Testing and Materials, New York, NY, pp. 60–89.

Stone, J.E., Scallan, A.M., 1967. The effect of component removal upon the porous structure of the cell wall of wood. II. Swelling in water and the fiber saturation point. Tappi 55 (10), 496–501.

Stone, J.E., Scallan, A.M., Abrahamson, B., 1968. Influence of beating on the cell wall swelling and internal fibrillation. Sv. Papperstidning 71 (19), 687–694.

Suresh, S., 1998. Fatique of materials, 2nd ed. Cambridge University Press.

Tynjälä, P., Kärenlampi, P.P., 2001. Spruce cell wall porosity—variation within annual ring and drying response. In: First International Conference of the European Society of Wood Mechanics, April 19–21, 2001, Lausanne, Swizerland, pp. 39–45.

Uhmeier, A., 1995. Some aspects on solid and fluid mechanics of wood in relation to mechanical pulping. Dissertation, Royal Institute of Technology, Stockholm.

Uhmeier, A., Salmén, L., 1996a. Influence of radial strain rate and temperature on the radial compression behavior of wet spruce. ASME JEMT, 118, 289–294.

Uhmeier, A., Salmén, L., 1996b. Repeated large radial compression of heated spruce. Nordic Pulp Paper Res. J. 11 (3), 171–176.

Williams, M.I., Landel, R.F., Ferry, J.D., 1955. Temperature dependence of relaxation mechanisms in amorphous polymers and other glass-forming liquids. J. Am. Chem. Soc. 77, 3901–3907.